

# Semisubmersible platforms with Steel Catenary Risers for Western Australia and Gulf of Mexico

Jun Zou\*

Houston Offshore Engineering, LLC, Houston, Texas, USA

(Received January 31, 2012, Revised April 13, 2012, Accepted April 23, 2012)

**Abstract.** Steel Catenary Risers (*SCR*) are the simplest and often the most economic solution compared to other riser types such as flexible pipe, riser towers, top tensioned risers, etc. The top of a *SCR* is connected to the host platform riser porch. The other end of the *SCR* connects to flowlines from subsea wells. The riser touchdown point (*TDP*), which is the location along the riser where contact with the sea floor first occurs, exhibits complex behaviors and often results in compression and fatigue related issues. Heave dynamic responses of semisubmersibles in extreme and operating sea states are crucial for feasibility of *SCR* application. Recent full field measurement results of a deep draft semisubmersible in Hurricane Gustav displayed the considerable discrepancies in heave responses characteristics between the measured and the simulated results. The adequacy and accuracy of the simulated results from recognized commercial software should be examined. This finding raised the awareness of shortcomings of current commercial software and potential risk in mega investment loss and environmental pollutions due to *SCR* failures. One main objective of this paper is to attempt to assess the importance and necessity of accounting for viscous effects during design and analysis by employing indicator of viscous parameter. Since viscous effects increase with nearly third power of significant wave height, thus newly increased metocean criteria per *API* in central Gulf of Mexico (*GoM*) and even more severe environmental conditions in Western Australia (*WA*) call for fundamental enhancements of the existing analysis tools to ensure reliable and robust design. Furthermore, another aim of this paper is to address the impacts of metocean criteria and design philosophy on semisubmersible hull sizing in *WA* and *GoM*.

**Keywords:** *SCRs TDP*; terminal velocity; viscous effects; viscous parameter; diffraction parameter; heave motion *RAOs*; cancelation zone

---

## 1. Introduction

Steel Catenary Risers (*SCR*) are the most popular and economic solution in deep and ultra deep waters of *GoM*. The top of a *SCR* is connected to the host platform at riser porch located on pontoon and the other end is connected to flowlines on sea bed. Between these two points, the riser hangs in a catenary shape and the bottom portion is supported by the sea floor. The riser touchdown point (*TDP*), which is the location along the riser where contact with the sea floor first occurs, is a critical area for design. Jesudasen *et al.* (2004) presented design considerations of large diameter *SCRs* supported by Spar. A Moros *et al.* (2004) addressed the use of *SCRs* with a semisubmersible in deep water prospects in *GoM*. It has been widely known that heave motions of a Spar is typically

---

\*Corresponding author, Dr., E-mail: [jzou@houston-offshore.com](mailto:jzou@houston-offshore.com)

better than a semisubmersible due to its 150m plus draft. Thus, *SCRs* hosted by a semisubmersible should be more carefully examined.

The common commercial software employed for numerical simulations of a semisubmersible are diffraction theory based which inherits to neglect viscous effects. It has been extensively studied in the past two to three decades the importance of accounting for viscous effects for fixed and floating structure to ensure drifting forces having been captured adequately, (Ferretti and Berta 1980, Chakrabarti 1984, Prinkster *et al.* 1993, Dev 1996, Dev and Pinkster 1997, Berthelsen *et al.* 2009). All studies, as best of knowledge, focused on surge/sway drifting forces which were essential for station keeping and mooring design of a semisubmersible. None of them addressed the importance of viscous effects on heave dynamic motions since the early generation semisubmersibles were mainly for drilling operations and not for productions. The design requirements for drilling operation and productions are considerably different since a semisubmersible designed for production has to be moored in production site for 20-30 years. Thus, 100-year hurricanes as well as 1,000-year hurricanes might be experienced during its service life. A drilling semisubmersible can be moved away if a reduced extreme event, such as 10-year hurricane, is approaching. Ma *et al.* (2010) first pointed out there are considerable discrepancies between the measured and the simulated heave responses based on full field measurements of a deep draft semisubmersible in *GoM*. Thus, interest and necessity of viscous effects on heave motions have been raised in order to adequately simulate physical phenomena and how to account for viscous effects in analysis tools to ensure reliable and robust results has been called for.

In the past studies, the “viscous parameter” ( $R_v = H/D$ ) and the “diffraction parameter” ( $R_d = \kappa * D$ ) have been used as a measure to determine the importance of the viscous/diffraction effect, where  $H$  stands for wave height,  $D$  denotes diameter of a cylinder and  $\kappa$  represents wave number. The larger “viscous parameter” is, the smaller “diffraction parameter” will be. In this study, definitions of viscous parameter and diffraction parameter are modified slightly,  $H$  is maximum wave height ( $1.86 * H_s$ ) for irregular waves and  $D$  is either diameter for a cylinder column or width for a square column.  $H_s$  means significant wave height for irregular waves.

In this paper, an attempt has been taken to assess the importance and necessity of accounting for viscous effects for heave responses during design and analysis by employing indicator of viscous parameter. It is essential for a semisubmersible with large diameter *SCRs* in harsh environmental conditions.

There have been several recent noteworthy deepwater discoveries in offshore Western Australia (*WA*). This region is remote and is known for both its harsh environment and unique soil conditions. These factors are essential design concerns as they can negatively influence the economics and risks associated with floating production platforms.

Large operating sea states with long swell periods present additional challenges for platform installation, and the remoteness of this region contributes to high mobilization costs for installation vessels. Quayside integration is therefore a desired feature of the hull concept to eliminate offshore mating and help reduce the cost and schedule risks associated with long offshore installation campaigns. One aim of this paper is to address the impacts of metocean criteria and design philosophy on semisubmersible hull sizing in *WA* and *GoM*.

This paper has been outlined as follows: first, design challenges for a floater with *SCRs* in large diameter are highlighted and addressed; second, comparisons of metocean conditions of the central *GoM* region and generic *WA* are briefly described; third, analysis results of a submersible in extreme and operating conditions of *WA* and *GoM* are presented; fourth, discussions on key design

aspects are addressed and finally, conclusions are drawn.

## 2. Design challenges of a floater with SCRs

To ensure the feasibility of large diameter SCRs for a floater, SCR strength and fatigue requirements have to be met in both extreme and operating sea states. The touchdown point (TDP) of an SCR exhibits complex behavior which may result in compression for extreme sea states and fatigue issues in operating sea states. Key design challenges are highlighted in Sections 2.1 to 2.4.

### 2.1. Terminal velocity

Terminal velocity per definition by McCann (2003) is reproduced in Eq. (1).

$$V_{TERM} = \sqrt{2mg / (C_D \cdot \rho \cdot D_{DRAG})} \quad (1)$$

where  $mg$  is the apparent weight of the pipe including internal fluid,  $C_D$  is the normal drag coefficient,  $D_{DRAG}$  is drag diameter, and  $\rho$  is water density. It is obvious from Eq. (1) that terminal velocity is SCR property depended and is independent of field location.

McCann *et al.* (2003) had investigated SCR TDP compression and global buckling issues and found terminal velocity is an important parameter. Furthermore, the non-dimensional parameter of  $V_{HT}$  ( $V_{HANGOFF}/V_{TERM}$ ) is recommended by McCann *et al.* (2003) to be utilized as a useful measure for assessing whether compression (buckling) will be an issue.  $V_{HANGOFF}$  is the vertical velocity of the SCR hang off point. TDP compression (buckling) may occur when  $V_{HT}$  is equal to or larger than 1.0.

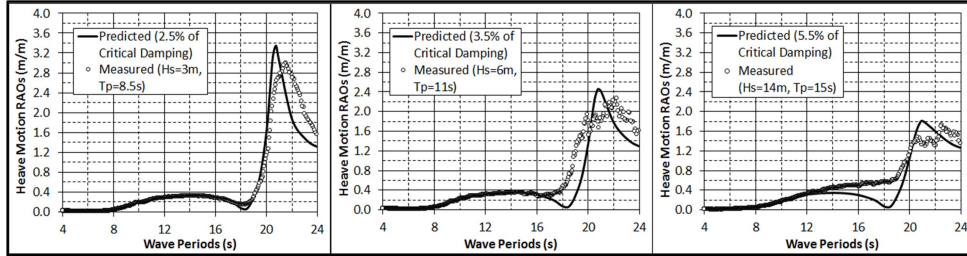
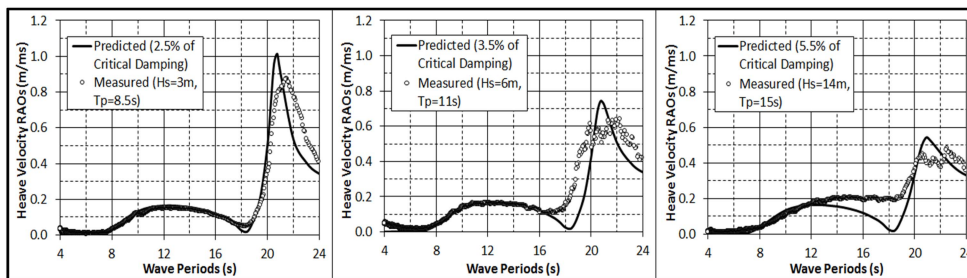
### 2.2. Hang off velocity

Vertical motion at the SCR porch is a combination of both platform heave, and vertical motions induced by roll/pitch motions. As the hang off location moves away from the center of rotation, the vertical motions due to roll/pitch increase significantly. Therefore, the hang off of catenary risers a greater distance away from platform center will experience more severe motions. This is especially true for extreme sea states.

Hang off velocity of the SCR is directly tied to host platform motions. Hang off velocity is a function of platform vertical motion at the SCR porch which consists of, (a) heave motion at the platform center, and (b) vertical motions due to roll and pitch motions. Therefore, by directly reducing platform heave, roll and pitch motions, and the lever arm from the platform center to the hang off location,  $V_{HANGOFF}$  will be reduced. Vertical motions due to platform rotations are significant during extreme events, and relatively small for fatigue sea states. Therefore, in order to improve SCR TDP fatigue life, one should focus on optimizing the platform's heave motions.

### 2.3. Viscous effects on heave motions and velocities

Wave basin model tests of a deep draft semisubmersible platform with square column 14 m, column central to central spacing 52 m and draft 33 m have been performed to investigate viscous

Fig. 1 Heave motion *RAOs* - predicted vs. measuredFig. 2 Heave velocity *RAOs* - predicted vs. measured

effects on heave response characteristics. Three wave only cases, (1)  $H_s = 3$  m,  $T_p = 8.5$  s; (2)  $H_s = 6$  m,  $T_p = 11$  s and (3)  $H_s = 14$  m,  $T_p = 15$  s, were tested and heave motion *RAOs* of the measured and the predicted are illustrated in Fig. 1. The heave motion velocity *RAOs* derived from heave motion *RAOs* by first derivative of heave motions. Since the heave accelerations have been directly measured, the procedure for deriving velocity *RAOs* from motion *RAOs* have been verified against the measured acceleration *RAOs*. The heave velocity *RAOs* for corresponding sea states are presented in Fig. 2.

The viscous parameters of these three irregular waves based on modified definition are 0.4, 0.8 and 1.86 respectively. The predicted results are based on diffraction theory and additional damping, 2.5%, 3.5% and 5.5% of critical damping were added correspondingly to cases 1, 2, and 3 to match the peaks around heave natural period.

It has been observed that cancellation zone around 18 seconds in predicted heave motion *RAOs* remains unchanged regardless additional damping variations. For the predicted results, only those near peaks varied when additional damping is changing. The other portion of the curve, say 20 seconds or less, remains unchanged. The common practices for current industry are just adding additional damping to which has been proven to be inadequate. The correct way to capture the viscous effects on heave motion and velocity responses is to add viscous excitation forces and damping into motion equation simultaneously. Calculations of the contributions of viscous excitation forces and associated viscous damping on heave responses are equally important to yield an accurate prediction. In fact, viscous damping in extreme sea states is relatively large compared radiation wave damping from diffraction theory. For the current commercial software, the feature to model viscous effects properly on heave responses has not been well established and valid so far.

It has been seen from Figs. 1, 2, and 3 to match the peaks around heave natural period.

- For small sea state, viscous parameter,  $R_v = 0.4$ , the predicted agreed well with the measured even including cancellation zone;

Table 1 Comparison of standard deviation and maximum of heave motions - predicted vs. measured

Sea states	Heave standard deviation			Maximum dynamic heaves		
	Predicted	Measured	Relative	Predicted	Measured	Relative
	m	m	%	m	m	%
	$A$	$B$	$(B-A)/A*100$	$C$	$D$	$(D-C)/C*100$
Case 1*	0.088	0.090	2.7%	0.351	0.375	7.0%
Case 2**	0.336	0.366	8.9%	1.344	1.540	14.6%
Case 3***	1.177	1.422	20.8%	4.706	5.804	23.3%

\*Case 1,  $H_s = 3$  m,  $T_p = 8.5$  s; \*\*Case 2,  $H_s = 6$  m,  $T_p = 11$  s; \*\*\*Case 3,  $H_s = 14$  m,  $T_p = 15$  s

Table 2 Comparison of standard deviation and maximum of heave velocities – predicted vs. measured

Sea states	Velocity standard deviation at CG			Maximum heave velocity at CG		
	Predicted	Measured	Relative	Predicted	Measured	Relative
	m	m	%	m	m	%
	$A$	$B$	$(B-A)/A*100$	$C$	$D$	$(D-C)/C*100$
Case 1*	0.056	0.057	2.5%	0.223	0.232	4.4%
Case 2**	0.186	0.201	8.4%	0.744	0.830	11.5%
Case 3***	0.491	0.591	20.4%	1.963	2.414	23.0%

\*Case 1,  $H_s = 3$  m,  $T_p = 8.5$  s; \*\*Case 2,  $H_s = 6$  m,  $T_p = 11$  s; \*\*\*Case 3,  $H_s = 14$  m,  $T_p = 15$  s

- For medium sea state, viscous parameter,  $R_v = 0.8$ , the predicted agreed well with the measured when wave periods are 17 seconds or less. The moderate deviations between the predicted and the measured have been observed for wave periods 17 seconds or higher, up to heave resonant period;
- For large sea state, viscous parameter,  $R_v = 1.86$ , the predicted agreed well with the measured only limited to wave periods 12 seconds or less. The large deviations between the predicted and the measured have been noticed for a wider range of wave periods.

It is obvious that the deviations strongly depended on viscous parameters. For  $R_v < 0.5$ , the predicted heave motion  $RAOs$  agree very well with the measured results including cancellation zone; for  $0.5 < R_v < 1.0$ , moderate deviations have been observed and for  $R_v > 1.0$ , the large deviations have been noticed. In addition, the deviation starts early (shorter wave period) when viscous parameter is increasing. This phenomenon clearly indicates the importance of viscous effects on heave responses especially for high seas.

The comparisons of standard deviation and maximum of heave motion and heave velocity of the predicted and measured in various sea states are given in Tables 1 and 2 respectively.

Again, the findings from Figs. 1 and 2 are further verified from Tables 1 and 2. The extreme motions and velocities of a semisubmersible in extreme sea states are seriously under-estimated which will result in seriously under-estimating  $SCRs$   $TDP$  compression and potentially buckling problem.

#### 2.4 Vertical water particle velocities

To estimate viscous effects on heave responses, the relative vertical velocities on bottoms of pontoons/columns are needed. The relative vertical velocity is the vector sum of the platform vertical velocity and vertical water particle velocity at bottom of pontoon. The measured wave elevation time series were employed to calculate the particle velocity time series at various depths below the mean water level (*MWL*). Since vertical water particle velocity was the only interest for this study, how to accurately predict horizontal particle velocity will not be addressed herein.

The measured wave elevation time series  $\eta(t)$  were decomposed by using *FFT* and both wave elevation amplitude and phase spectra were kept for generating vertical particle velocity amplitude and phase spectra. Then, *IFFT* was applied to generate vertical particle velocity time series at the specified depth below. The equations involved in the calculation are listed as follows

$$\eta(t) = \sum_{i=1}^n Amp_e(i) * \cos(Phy_e(i)) \quad (2)$$

where,  $\eta(t)$  represents the measured wave elevation time series and  $Amp_e(i)$  and  $Phy_e(i)$  are wave elevation *i*-th component amplitude and phase. Thus, an irregular wave elevation time series was decomposed into summation of “*n*” components of regular waves. An *i*-th regular wave component has amplitude  $Amp_e(i)$  and phase  $Phy_e(i)$ . For a regular wave in deep water, vertical particle velocity at depth *z* is denoted as follow

$$\kappa_i = \omega_i / g \quad (3)$$

$$v_z(i) = \omega_i * Amp_e(i) * e^{\kappa_i z} \sin(Phy_e(i)) \quad (4)$$

$$Amp_v(i) = \omega_i * Amp_e(i) * e^{\kappa_i z} \quad (5)$$

$$Phy_v(i) = Phy_e(i) \quad (6)$$

where,  $\kappa_i$  is the wave number of *i*-th component regular wave in Eq. (3),  $v_z(i)$  is the vertical particle velocity of *i*-th regular wave component at depth *z* in Eq. (4),  $Amp_v(i)$  is the vertical particle amplitude and  $Phy_v(i)$  is the phase of the corresponding regular wave in Eqs. (5) and (6) respectively. Once vertical velocity amplitude and phase spectra were obtained, *IFFT* can be applied and vertical particle velocity time series at depth *z* can be generated. Since the vertical particle velocities involved in this study are at the *MWL* or below, no stretch method was employed. The above described method had been validated against the measurements, Kim and Zou (1995), Choi (2005). Thus, it is believed to be adequate for this study.

The maximum vertical water particle velocity profiles along vertical axis from *MWL* down to 48.0 m below are illustrated in Fig. 3.

Maximum platform heave velocities, vertical water particle velocities at -33 m and relative vertical velocities and relative vertical velocity square are summarized in Table 3 and maximum relative vertical velocity at -33 m square as a function of significant wave height is shown in Fig. 4. The best fitting trend line as well as best fitting equation and R-squared value were also displayed in Fig. 4.

The vertical viscous force on one of pontoons/columns in Morison equation form is denoted as

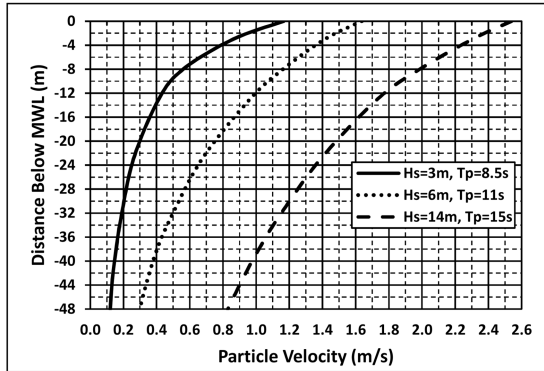


Fig. 3 Vertical water particle velocity profiles

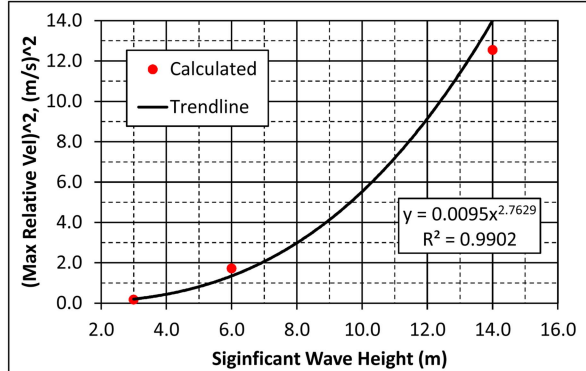


Fig. 4 Maximum relative velocity square as a function of significant wave height

Table 3 Summary of maximum heave, vertical particle and relative velocities

$H_s$	Maximum Heave velocity	Maximum vertical Particle velocity at -33 m	Maximum relative Vertical velocity at -33 m	Maximum relative Vertical velocity at -33 m squared
$m$	$m/s$	$m/s$	$m/s$	$(m/s)^2$
$A$	$B$	$C$	$B+C$	$(B+C)^2$
3.0	0.232	0.184	0.417	0.174
6.0	0.830	0.482	1.311	1.719
14.0	2.414	1.128	3.542	12.543

follows

$$F_{viscous}(t) = \frac{1}{2} \rho C_d A v_{rel} |v_{rel}| \tag{7}$$

where,  $F_{viscous}$  stands for vertical viscous forces;  $\rho$  represents sea water density;  $C_d$  means vertical drag coefficient;  $A$  is either pontoon or column vertical project area and  $v_{rel}$  denotes vertical relative velocity.

From Eq. (7), it is obvious  $F_{viscous} \propto v_{rel}^2$  and from Fig. 4, it has been found  $v_{rel}^2 \propto H_s^{2.76}$  since wave peak period is another parameter which has not been factored into equation yet; thus one can derive the following relationship

$$F_{viscous} \propto H_s^{2.76} \tag{8}$$

From Eq. (8), viscous forces are proportional to nearly third power of significant wave height (nearly cubic not quadratic). For new central *GoM*, 100-year and 1,000-year waves (API 2007) and *WA*, 100-year and 10,000-year waves, larger viscous effects are anticipated and it is even more essential to account for viscous effects properly in order to have a reliable and robust design in these regions.

### 3. Metocean of Western Australia and Gulf of Mexico

#### 3.1 Extreme sea states

Generic *WA* metocean criteria are compared to the central region of the Gulf of Mexico (*API* 2007). Results are summarized in Table 4. The corresponding waves and winds are found to be very close. In terms of design criteria, 10,000-yr return period (*RP*) conditions are typically selected as a survival check in *WA*, while 1,000-yr *RP* conditions are normally recommended per *API* for the Gulf of Mexico. Because of differences in design philosophy between *WA* and the *GoM*, column freeboard must be increased accordingly, and the heave natural period for a semisubmersible should be shifted at least 1 sec to the longer side. Consideration of the 10,000-yr conditions for a survival check in *WA* has a significant influence on platform configuration and sizing.

#### 3.2 Wave scatter diagrams

To better understand the influence of operating sea states on *SCR* fatigue at the touchdown point, generic *WA* and typical *GoM* wave scatter diagrams are plotted and shown in Fig. 5.

For the generic *WA* wave scatter diagram in Fig. 5, there exist a large percentage of waves in the

Table 4 Comparison of extreme waves and winds of generic *WA* and central *GoM*

Parameters	Units	Generic <i>WA</i>			Central <i>GoM</i>		
		10,000-yr	1,000-yr	100-yr	10,000-yr	1,000-yr	100-yr
$H_s$	m	22.5	20.5	16.8	22.1	19.8	15.8
$T_p$	sec	18.1	17.1	15.3	18.2	17.2	15.4
Hourly wind	m/s	68.5	62.0	50.0	67.2	60.0	48.0

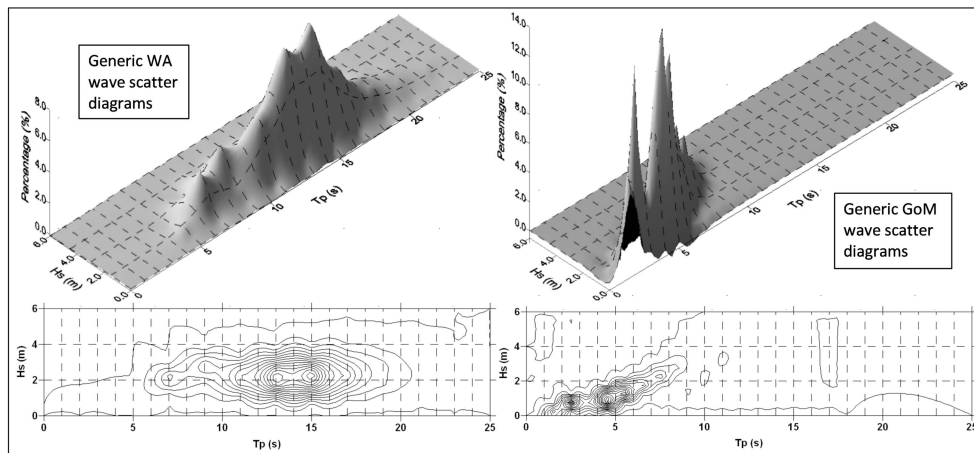


Fig. 5 Generic *WA* and typical *GoM* wave scatter diagrams

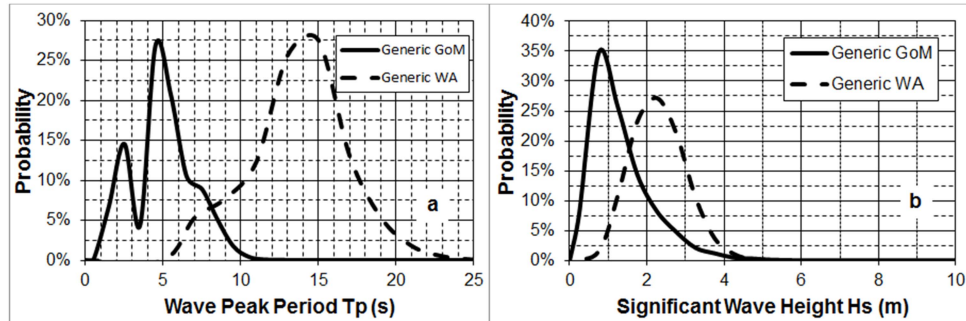


Fig. 6 Generic *WA* and *GoM* wave scatter diagram as a function of  $T_p$  (a) and  $H_s$  (b)

approximate range of 1 to 4 m  $H_s$  and 8 to 17 sec  $T_p$ . There are almost no waves with  $T_p$  less than 8 sec. In contrast, the *GoM* wave scatter diagram shows a large percentage of waves in the approximate range of 0 to 4 m  $H_s$  and 1 to 10 sec  $T_p$ . There are almost no waves with  $T_p$  larger than 10 sec.

The differences in these two wave scatter diagrams are important as they directly impact the floater hull configuration, heave motion contributions to *SCR* fatigue life and installation cost. These are addressed in detail in later sections.

*WA* and *GoM* wave scatter diagram data are shown in Fig. 6 as percentages of occurrence as a function of both wave peak period  $T_p$  (left) and significant wave height  $H_s$  (right).

The different characteristics of the *WA* and *GoM* wave scatter diagrams are further displayed in this figure. The key aspects which affect hull configuration are as follows:

- For the *GoM*, the dominant wave peak period occurrence is approximately 4.5 sec. The probability of occurrence dramatically reduces out to approximately 10 sec and essentially goes to zero after that.
- For *WA*, the dominant wave peak period occurrence is approximately 14 sec. There are near zero occurrences of wave peak periods below 5 sec and above 25 sec. It should be noted that wave peak periods beyond 20 sec presents a considerable design challenge for floaters such as semisubmersible and Spar. A more in-depth discussion follows in a later section.
- The dominant occurrence of significant wave height in the *GoM* is approximately 0.8 m. The probability of occurrence dramatically reduces out to approximately 4 m and essentially goes to zero beyond 5 m.
- For *WA*, the dominant occurrence of significant wave height is approximately 2.3 m which is more than twice that seen in the *GoM*. Similarly, the occurrence of significant wave height drops dramatically out to approximately 4 m and essentially goes to zero beyond 5 m.

## 4. Analysis results

### 4.1 General

The host platform used for this study is a pair-column semisubmersible platform as illustrated in Fig. 7 and key figures of hull configuration are summarized in Table 5. The description of advantages of this hull form over typical deep draft semisubmersible hull has been presented in Zou and Chianis (2011) and

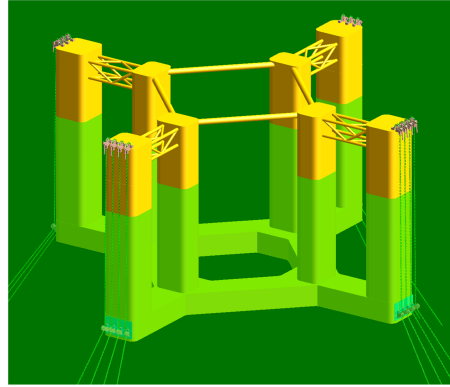


Fig. 7 A pair-column semi-submersible platform hull and mooring configuration

Table 5 Key figures of the pair-column semi-submersible platform

Items	Units	Data
Draft	(m)	50.0
Displacement	(mt)	75,489
Inner Column Length x Width	(m)	$9.1 \times 13.0$
Inner Column c/c Span	(m)	50.3
Main Pontoon Width $\times$ Height	(m)	$12.0 \times 8.0$
Outer Column Length $\times$ Width	(m)	$11.0 \times 13.0$
Connecting Pontoon Width $\times$ Height	(m)	$13.0 \times 8.0$
Distance between Inner/Outer Columns	(m)	15.0
Total Weight	(mt)	70,535
SCRs + Mooring Vertical Loads	(mt)	4,955
Vertical C.G. from base (Mass only)	(m)	27.34
Roll Radii of Gyration, $K_{xx}$	(m)	41.7
Pitch Radii of Gyration, $K_{yy}$	(m)	41.5
Yaw Radii of Gyration, $K_{zz}$	(m)	43.3
GMtc (Free Surface Correction, Mass VCG)	(m)	8.2

thus omitted here.

This concept won a competition hosted by RPSEA (Research Partnership to Secure Energy for America) in 2009. A comprehensive and systematic study including wind tunnel and wave basin model tests has been funded in order to mature the concept and prepare it for application to a major capital project. RPSEA continued to support this concept and funding on extensive Vortex Induced Motions (VIM) model tests will be provided in 2013.

#### 4.2 Extreme heave responses in WA and GoM

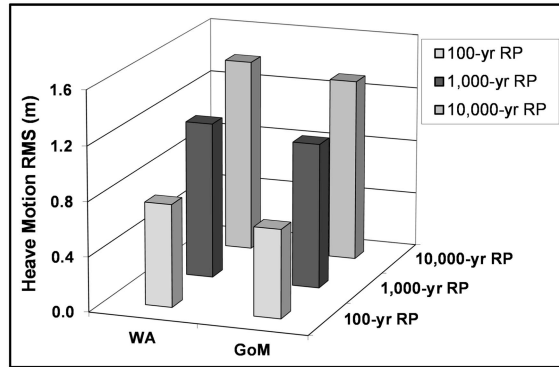


Fig. 8 Comparison of heave motion *RMS* in *WA* and *GoM*

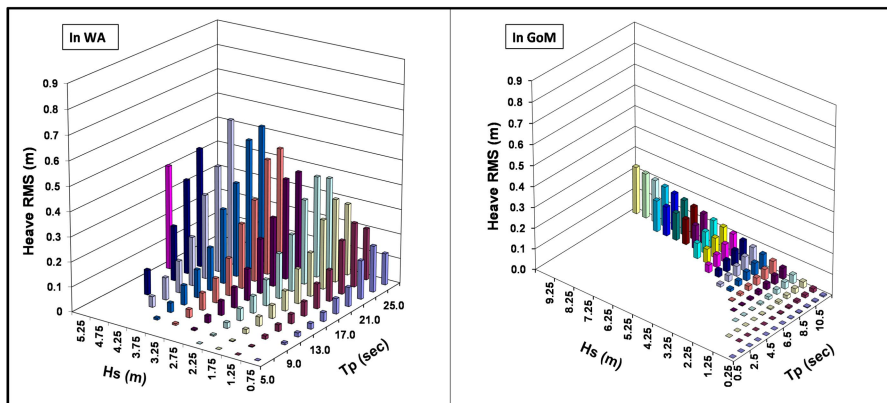


Fig. 9 Heave *RMS* in fatigue seas of *WA* and *GoM*

The heave responses in 100-, 1,000- and 10,000-yr RP events of *WA* and *GoM* as described in Table 4 are shown in Fig. 8. The *RMS* heave motions in *GoM* are slightly smaller than the corresponding *RMS* heave motions in *WA*. However, 1,000-yr *RP* events in *GoM* are survival conditions recommended by *API* while 10,000-yr *RP* events in *WA* are typically selected as survival conditions per Australia traditional design philosophy. Due to altering design philosophy in *WA*, 10,000-yr *RP* events are becoming governing cases for maximum allowable heave motion requirements in order to be lower than terminal velocity to avoid compression and potential bulking at *SCR TDP*. In addition, minimum airgap (minimum column freeboard) requirements are also governed by 10,000-yr *RP* events. The impacts on hull sizing are considerably high.

#### 4.3 Heave responses in fatigue seas of *WA* and *GoM*

Heave responses in fatigue sea states of *WA* and *GoM* are illustrated in Fig. 9. Distinct response characteristics have been found.

Heave responses in *GoM* need not be shown for wave peak periods above 11.5 sec based on Fig. 5 which shows that the probability of *GoM* fatigue seas is near zero for wave periods longer than 11.5 sec.

From Fig. 9, it is seen that heave motions are nearly zero for the dominant probability around 4.5 sec. Also, for  $H_s = 9.75$  m and  $T_p = 11.5$  sec, heave motions are about half that for  $H_s = 5.25$  m

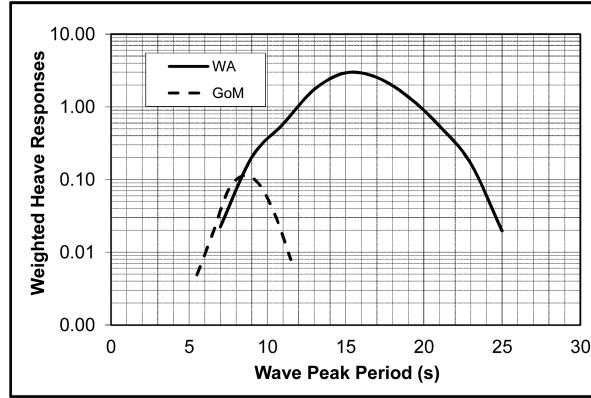


Fig. 10 Weighted heave responses in *WA* and *GoM* fatigue seas

and  $T_p = 17.0$  sec. This indicates that wave peak period has a more pronounced effect on heave motions than significant wave height.

#### 4.4. Weighted heave motions in fatigue seas of *WA* and *GoM*

Heave responses of generic fatigue seas in *WA* and *GoM* are presented in Section 4.3 and the probability corresponding to each fatigue sea state as illustrated in Fig. 5. Weighted heave motion is defined as heave motion multiplied by the corresponding probability of that sea state. Fig. 10 shows the sum of all weighted heave motions corresponding to the same  $T_p$ .

The above figure shows as follows

- The largest weighted heave in *WA* is about 30 times higher than the largest weighted heave in the *GoM*. This indicates that it is much more challenging to satisfy *SCR* fatigue life requirements in *WA* than in the *GoM*. Because of this, hull configurations in *WA* and *GoM* will be considerably affected.
- The weighted heaves for *WA* peak at 15.0 sec while the weighted heaves for *GoM* peak at 8.5 sec. This clearly indicates the long swell effects on heave responses of a semisubmersible which will translate to *SCRs* at *TDP* and impact the fatigue significantly.

## 5. Discussions

### 5.1 Viscous effects on heave responses

Viscous effects on heave responses have been closely studied. The attempt has been taken to assess the importance and necessity of accounting for viscous effects during design and analysis by employing indicator of viscous parameter.

From correlation analysis of physical wave basin test results, it has clearly confirmed that the deviations strongly depended on viscous parameter ( $R_v$ ). For  $R_v < 0.5$ , the predicted heave motion *RAOs* agree very well with the measured results including cancellation zone; for  $0.5 < R_v < 1.0$ , moderate deviations have been observed and for  $R_v > 1.0$ , the large deviations are anticipated. In addition, the deviation starts early (shorter wave period) when viscous parameter is increasing.

For current commercial software diffraction theory based, the typical way by solely adding additional damping to account for viscous effects for heave responses have been proven to be inadequate to capture the characteristics of heave responses in high seas. Including proper viscous excitation forces and damping are equally critical to ensure reliable and robust design and analysis.

After Hurricane Katrina and Rita, metocean criteria increased considerably in *GoM* per latest *API*. In addition, active explorations have extended and reached more severe environmental region, such as Western Australia. Since viscous effects increase with nearly third power of significant wave height, it becomes more essential and necessary to account for viscous effects properly on heave dynamic responses of semisubmersibles with *SCRs* designed for these regions.

## 5.2 Hull configurations in *WA* and *GoM*

The extreme sea states of *WA*, as shown in Table 4, are slightly worse than the corresponding sea states in central *GoM*. However, 10,000-yr events are selected as survival conditions in *WA* common offshore design practice while 1,000-yr events are recommended as survival cases per *API*. There are more than 30% higher in *WA* if extreme heave motion *RMS* value in *WA* 10,000-yr events is compared with that in *GoM* 1,000-yr events.

Due to altering design philosophy in *WA*, 10,000-yr *RP* events are becoming governing cases for maximum allowable heave motion requirements in order to be lower than terminal velocity to avoid compression and potential bulking at *SCR TDP*. In addition, minimum airgap (minimum column freeboard) requirements are also governed by 10,000-yr *RP* events. The impacts on hull sizing are considerably high. A brief summary is highlighted as follows:

(a) Hull draft for application in the *GoM* can be 10 m less than in *WA* due to the reduced required *SCR* porch vertical velocity

(b) Hull freeboard for application in the *GoM* can be 3 m less than in *WA* due to the reduced wave crest heights

(c) Based on the items (a) and (b), column span for application in the *GoM* can be 5 to 10 m less than in *WA*

(d) Based on item (c), deck steel weight for application in the *GoM* can be 15 to 25% less than in *WA* due to the reduced column/column spacing

(e) Based on all above items, hull displacement for application in the *GoM* can be 25 to 35% less than in *WA*

(f) Based on all above items, mooring systems for application in the *GoM* can have either fewer mooring lines and/or smaller line sizes than those in *WA*

(g) Based on all above items, the hull for application in the *GoM* is easier for construction, transportation and installation than in *WA*

(h) Based on all above items, the hull for application in the *GoM* is significantly more economic than in *WA* for carrying the same topsides payload

## 6. Conclusions

Viscous effects on heave dynamic response characteristics of a semisubmersible have been investigated and identified. Viscous parameter can be a useful indicator to measure the importance

and necessity of viscous effects. Simultaneously including viscous excitation forces and damping are crucial to capture the heave dynamic response characteristics in high seas. There are more pronounced viscous effects when one designs a semisubmersible in central *GoM* and/or *WA* since viscous effects increase with nearly third power of significant wave height.

The remote region of Western Australia has several unique features which complicates the development of economic and low risk deepwater floating production platforms. These characteristics include metocean and soil conditions, 10,000-yr survival criteria, high labor and mobilization costs, etc.

Although wet tree developments with Steel Catenary Risers are well-proven in the Gulf of Mexico, their application to *WA* is relatively new and will prove to be a challenge for acceptable *SCR* performance. This paper has identified the differences between *GoM* and *WA* metocean conditions and how *SCR* performance is influenced by both operational and extreme sea states for each. Furthermore, it has found the hull for *GoM* is considerably more economic than hull in *WA* for carrying the same topsides payload.

## Acknowledgements

The author would like to express appreciation to the management of Houston Offshore Engineering (HOE) for supporting semi-submersible developments and related hydrodynamic researches.

## References

- A Moros, E.P.A., Cerkovnik, M., Fang, J. and Rasmussen, J. (2004), *The use of SCRs with semi for the development of deep water prospects*, DOT, Nov 30<sup>th</sup> Dec 2<sup>nd</sup>.
- API 2INT-MET (2007), *Interim guidance on hurricane conditions in the Gulf of Mexico*, 1<sup>st</sup> Ed., (draft), May.
- Berthelsen, P.A., Baarholm, R., Pakozdi, C., Stansberg, C.T., Hassan, A., Downle, M. and Incecik, A. (2009), "Viscous drift forces and responses on a semisubmersible platform in high waves", *Proceedings of the International Conference on Ocean, Offshore and Arctic Engineering (OMAE)*.
- Chakrabarti, S.K. (1984), "Steady drift force on vertical cylinder – viscous vs. potential", *Appl. Ocean Res.*, **6**(2), 73-82.
- Choi, H.J. (2005), *Kinematics measurements of regular, irregular, and rogue waves by PIV/LDV*, Ph. D. Dissertation, Ocean Engineering Program, Texas A&M University.
- Dev, A.K. (1996), *Viscous effects in drift forces on semi-submersibles*, Ph. D. Dissertation, Delft University of Technology.
- Dev, A.K. and Pinkster (1997), "Viscous mean and low frequency drift forces on semi-submersibles", *Proceedings of the International Conference on Behavior of Offshore Structures, BOSS'97* (8<sup>th</sup>), July 7-10.
- Ferretti, C. and Berta, M. (1980), "Viscous effects contribution to the drift forces on floating structures", *Proceedings of the International Symposium of Ocean Engineering and Ship Handling, SSPA*, Gothenburg, Sweden.
- Jesudasan, A.S., McShane, B.M., McDonald, W.J., Vandenbossche, M. and Souza, L.F. (2004), "Design considerations particular to SCRs supported by Spar buoy platform structures", *Proceedings of the Offshore Technology Conference (OTC)*.
- Kim, C.H. and Zou, J. (1995), "A universal linear system model for kinematics and forces affected by nonlinear irregular waves", *Int. J. Offshore Polar.*, **5**(3), 166-170
- Ma, W., Lee, M.Y., Tule, J. and Zou, J. (2010), *Full scale response verification of a deep draft semisubmersible*

- production platform*, Deepwater Offshore Technology (DOT).
- McCann, D., Smith, F. and O'Brien, P. (2003), "Guidelines for compression modeling in flexible risers for deepwater applications", *Proceedings of the Offshore Technology Conference*, Houston, Texas, 5 May- 8 May.
- Pinkster, J.A., Dercksen, A. and Dev, A.K. (1993), "Hydrodynamic aspects of moored semisubmersibles and TLP's", *Proceedings of the Offshore Technology Conference*, Houston, Texas, 3 May-6 May.
- Zou, J. and Chianis, J. (2011), "Paired-column semisubmersible platform for wet tree with steel catenary riser application in offshore Western Australia", *Proceedings of the International Conference on Ocean System Engineering*, Seoul, Korea.